
The FFT Strikes Again: An Efficient Alternative to Self-Attention

Jacob Fein-Ashley

University of Southern California
feinash1@usc.edu

Rajgopal Kannan

DEVCOM Army Research Office
rajgopal.kannan.civ@army.mil

Viktor Prasanna

University of Southern California
prasanna@usc.edu

Abstract

Conventional self-attention mechanisms exhibit quadratic complexity in sequence length, making them challenging to scale for long inputs. We present **FFTNet**, an adaptive spectral filtering framework that uses the Fast Fourier Transform (FFT) to achieve global token mixing in $\mathcal{O}(n \log n)$ time. By mapping inputs into the frequency domain, FFTNet exploits orthogonality and energy preservation—guaranteed by Parseval’s theorem—to efficiently model long-range dependencies. Our main theoretical contributions include 1) An adaptive spectral filter that highlights salient frequency components, 2) A hybrid scheme combining local windowing with a global FFT branch, 3) Nonlinear feature transformations applied in both the frequency and token domains. Experiments on Long Range Arena and ImageNet validate our theoretical insights and demonstrate superior performance over fixed Fourier-based and standard attention models.

1 Introduction

Conventional self-attention mechanisms capture global interactions through explicit token-pair computations, resulting in quadratic complexity $\mathcal{O}(n^2)$. This high cost becomes prohibitive for tasks involving lengthy sequences, such as long-context language modeling or large-scale image processing.

In this paper, we introduce an adaptive spectral filtering framework that leverages the Fast Fourier Transform (FFT) to perform global token mixing with $\mathcal{O}(n \log n)$ efficiency. By converting the input sequence into the frequency domain, we harness orthogonal frequency components to naturally capture long-range dependencies. This frequency-domain representation not only reduces computational overhead but also preserves the original signal’s energy due to Parseval’s theorem.

A distinguishing feature of our approach is a learnable spectral filter that modulates the Fourier coefficients based on a global context vector. This adaptive mechanism selects which frequency bands are most relevant, allowing the model to dynamically focus on critical components of the input. Additionally, introducing nonlinear activations to both the real and imaginary parts of the signal extends the representational capacity beyond linear transformations, enabling the model to capture more complex interactions.

Overall, our adaptive spectral filtering framework unifies the efficiency of FFT-based methods with a powerful, input-dependent spectral filter and nonlinear feature modulation. This combination offers a computationally efficient and expressive alternative to traditional self-attention, promising robust handling of long-range dependencies in various sequence modeling tasks.

2 Related Work

In this section, we review existing methods aimed at improving the efficiency of sequence models. We first discuss the complexity issues inherent in self-attention (Section 2.1), then highlight Fourier-based approaches (Section 2.2) and other approximation techniques (Section 2.3). We then examine orthogonal matrix decomposition methods (Section 2.5), and finally position our adaptive spectral filtering method within this landscape (Section 2.6).

2.1 Self-Attention Complexity

The original Transformer architecture Vaswani et al. [2017] uses pairwise dot-product attention, incurring a computational and memory cost of $\mathcal{O}(n^2)$, where n is the sequence length. As n grows, this quadratic complexity quickly becomes infeasible for long sequences in tasks such as language modeling and long-context document understanding.

2.2 Fourier-Based Mixing

Fourier-based approaches leverage the Fast Fourier Transform (FFT) Cooley and Tukey [1965] to achieve more efficient global mixing of tokens. FNet Lee-Thorp et al. [2022], for example, replaces the self-attention sublayer with a fixed Fourier transform, drastically lowering computational overhead. However, the use of a static transform limits its capacity to adapt to varying inputs or highlight task-specific frequency components.

Beyond language and vision tasks, Fourier-based methods have also proven effective in modeling physical processes governed by partial differential equations. Fourier Neural Operator (FNO) Li et al. [2021] demonstrates that neural architectures parameterized in the Fourier domain can learn solution operators for parametric PDEs, achieving resolution-invariant performance and fast inference. Although primarily designed for PDE modeling and simulation, FNO nonetheless highlights the broader potential of leveraging Fourier representations for efficient token mixing in deep learning applications.

In another line of work, Xu *et al.* Xu et al. [2020] propose learning-based frequency selection methods for large-scale vision tasks, showing that CNNs can be trained directly on partial frequency components while retaining high accuracy. Their approach offers a path to reducing data transmission overhead and computational costs without sacrificing performance.

2.3 Linear, Sparse, and Low-Rank Approximations

Beyond Fourier methods, several alternative strategies aim to reduce the cost of self-attention. Performer Choromanski et al. [2021] and linear transformer variants Katharopoulos et al. [2020] approximate the softmax attention matrix to achieve linear or near-linear complexity. Meanwhile, Reformer Kitaev et al. [2020], Linformer Wang et al. [2020], and BigBird Zaheer et al. [2020] employ sparse or low-rank approximations, extending the effective context length without paying the full quadratic price. Other approaches like Synthesizer Tay et al. [2020] and MLP-Mixer Tolstikhin et al. [2021] avoid explicit token-pair interactions, replacing them with fixed or learned mixing operations.

2.4 Convolution-Based Approaches

Another line of work replaces or augments self-attention with convolutional modules to capture long-range dependencies. Methods such as Hyena Poli et al. [2023] introduce a hierarchical, convolution-based framework that can scale to long input sequences while maintaining the expressive capacity of attention. Similarly, lightweight and dynamic convolutions Wu et al. [2019] have been proposed to reduce the cost associated with attention heads, learning per-feature or per-time-step kernels to approximate global interactions. Although these methods can exhibit favorable scaling compared to vanilla self-attention, they often rely on carefully designed convolutional architectures to handle very long contexts.

2.5 Orthogonal Matrix Decomposition Methods

Orthogonal (or unitary) transformations provide a powerful avenue for stable and efficient sequence modeling. A key advantage of orthogonal decompositions is their norm-preserving property, which can mitigate issues such as vanishing or exploding gradients Wisdom et al. [2016]. In the context of RNNs, unitary or orthonormal recurrent weights have been shown to preserve long-term dependencies while keeping representations stable Arjovsky et al. [2016], Lezcano-Casado and Martínez-Rubio [2019]. From another perspective, the discrete Fourier transform (DFT) itself is an orthonormal transformation (up to scaling) that can mix tokens globally without explicit pairwise attention.

The FFT-based approaches discussed above can be viewed as a special class of such orthonormal transforms, where the matrix is structured by the DFT. More general orthogonal transformations—whether learned or hand-crafted—have also been proposed to reduce complexity or enhance stability in modern architectures. These include fast variants of orthonormal transforms, often parameterized in ways that ensure orthogonality is preserved throughout training Lezcano-Casado and Martínez-Rubio [2019]. Within Transformers, adopting orthogonal or unitary blocks has been explored to stabilize training and capture global structure, although these methods may not always achieve the same $\mathcal{O}(n \log n)$ cost as the FFT. Nonetheless, they highlight a broad paradigm wherein structured or parameterized orthonormal decompositions serve as efficient global mixing mechanisms.

Recently, there has also been significant progress in state space modeling approaches for sequence tasks, exemplified by S4 and its extensions. More streamlined variants such as the Simplified State Space layer (S5) Smith et al. [2023] have demonstrated that parameterizing the state space system with a diagonal transition matrix can enable efficient parallel scans over the sequence dimension while preserving high performance. These developments underscore the ongoing push to find alternatives to self-attention that can handle long sequence lengths without sacrificing expressiveness.

2.6 Adaptive Spectral Filtering in Context

Our work diverges from both fixed Fourier-based schemes and the various attention approximations by incorporating a *learnable* filter in the frequency domain. This adaptive mechanism leverages the theoretical underpinnings of FFT-based transformations—including energy preservation via Parseval’s theorem—while permitting dynamic reweighting of salient frequency bands. Thus, our method maintains an $\mathcal{O}(n \log n)$ complexity yet provides richer expressivity than fixed spectral mixing approaches. In contrast to purely approximate or sparse attention mechanisms, adaptive spectral filtering offers a direct and theoretically grounded route to capture long-range dependencies efficiently.

Notably, our approach also differentiates itself from recent work such as Guibas et al. [2022], which introduces Adaptive Fourier Neural Operators (AFNO) for token mixing. While AFNO employs a block-diagonal structure for channel mixing and adaptive weight sharing, our method takes a distinct approach. Specifically, we compute a global context vector that directly modulates the Fourier coefficients via learnable scaling and bias parameters, followed by a nonlinear modReLU activation. This design not only preserves the computational advantages of FFT-based mixing but also enhances expressivity by dynamically emphasizing salient frequency bands based on the input. As such, our adaptive spectral filtering strategy offers a complementary alternative to AFNO, merging efficiency with adaptive, context-dependent feature modulation.

Overall, while approaches such as FNet, Performer, and sparse transformers demonstrate that either fixed or approximate token mixing can reduce computational overhead, our adaptive spectral filtering strategy uniquely merges the efficiency of the FFT with a learnable, input-dependent spectral filter. This provides a compelling combination of scalability and adaptability, which is crucial for complex sequence modeling tasks.

3 Adaptive Spectral Filtering Method

We present an *adaptive spectral filtering* framework that avoids explicit pairwise interactions while retaining global mixing capabilities. Rather than computing dot-product self-attention, this approach applies the discrete Fourier transform (DFT) to capture long-range dependencies in $\mathcal{O}(n \log n)$ time. By adaptively reweighting the resulting frequency components and then applying an inverse transform,

the method achieves an effective balance of expressive power and computational efficiency, backed by solid theoretical foundations.

3.1 Motivation

Traditional attention mechanisms incur quadratic cost in the sequence length n when computing pairwise token interactions. As n increases, this quickly becomes expensive. By contrast, the DFT naturally encodes global interactions in $\mathcal{O}(n \log n)$ time, since it decomposes the token sequence into orthogonal frequency components. To increase representational power, we introduce a learnable filter in the frequency domain that emphasizes or attenuates particular frequency bands based on a global context.

Why Local Windowing (or Wavelets)? While the global DFT branch is excellent for capturing large-scale dependencies, it can blur fine-grained or short-range signals. *Local windowing (STFT) is optional, but it can help* preserve the high-resolution structure within shorter segments. In fact, *wavelet transforms* can also be used here instead of or alongside STFT, offering a multi-resolution perspective that naturally adapts to local signal changes. When used, merging these *local* (STFT or wavelets) and *global* representations yields a model capable of both wide-ranging context and precise local detail. If purely global context suffices, one may omit local windowing or wavelet transforms altogether.

3.2 Method Description

Let $\mathbf{X} \in \mathbb{R}^{n \times d}$ be an input sequence of length n and embedding dimension d . Our method integrates both *global* and *local* spectral representations to capture wide-ranging dependencies and fine-grained context. The approach proceeds in five main steps:

1 Global Fourier Transform.

Apply the discrete Fourier transform (FFT) *across the entire sequence*:

$$\mathbf{F}_{\text{global}} = \text{FFT}(\mathbf{X}) \in \mathbb{C}^{n \times d},$$

which captures long-range dependencies without explicit pairwise comparisons.

2 Local Windowing (STFT) or Wavelets. (*Optional*)

In parallel, and *optionally*, perform a short-time Fourier transform (STFT) *or* a wavelet transform for local context:

1. **For STFT:** Partition the input \mathbf{X} into overlapping windows of length w . Let each window be denoted by $\mathbf{X}^{(m)} \in \mathbb{R}^{w \times d}$, where m indexes the window.
2. Apply a window function (e.g., Hann or Hamming) to each segment.
3. Compute the FFT for each window to obtain local frequency components:

$$\mathbf{F}_{\text{local}}^{(m)} = \text{FFT}(\mathbf{X}^{(m)}).$$

4. **Alternatively (Wavelets):** Decompose each local segment using a chosen wavelet family (e.g. Daubechies) to capture time-varying frequency information at multiple scales.

These local spectra or wavelet coefficients emphasize short-range patterns that might be blurred in a purely global transform. If the application does not require high-resolution local detail, this step can be omitted.

3 Merging Global and Local Representations.

To *maximize information flow* from both branches, we propose an *isometric fusion* approach in the frequency (or transform) domain. First, concatenate the global and local representations (spectra or wavelet coefficients) along their feature dimension:¹

$$\hat{\mathbf{F}} = [\mathbf{F}_{\text{global}} \parallel \mathbf{F}_{\text{local}}] \in \mathbb{C}^{n \times (2d)},$$

¹If multiple local windows exist, they may be pooled or aggregated (e.g. average or max) before concatenation, or one can apply a deeper fusion network to combine them.

where $\mathbf{F}_{\text{local}}$ can be a representative fusion of all local windows (or wavelet scales).²

Next, apply a learnable matrix $\mathbf{U} \in \mathbb{C}^{(2d) \times d}$ that fuses the concatenated features into a unified spectral representation:

$$\mathbf{F} = \hat{\mathbf{F}} \mathbf{U}.$$

In the simplest form, \mathbf{U} can be unconstrained and learned end-to-end. However, to *preserve* (and thus maximize) the signal energy from both branches, \mathbf{U} may be constrained to be *isometric* (or approximately isometric), satisfying $\mathbf{U}^* \mathbf{U} = \mathbf{I}$. This ensures that no information is lost during the fusion step, effectively providing a richer merge than a simple gating or element-wise sum.

Gating Instead of Concatenation (When Resources Are Limited). If memory or computational overhead from concatenation is a concern, one may *gate* the local and global transforms instead. For example, one can learn a scalar or vector gate $\sigma(\mathbf{c})$ (where \mathbf{c} is a global context) that modulates:

$$\hat{\mathbf{F}} = \sigma(\mathbf{c}) \odot \mathbf{F}_{\text{global}} + (1 - \sigma(\mathbf{c})) \odot \mathbf{F}_{\text{local}}.$$

In this case, the fusion dimension is unchanged and can be more lightweight, albeit at the cost of discarding some of the richer information that the concatenation-based approach retains.

4 Adaptive Spectral Filtering.

Compute a global context vector

$$\mathbf{c} = \frac{1}{n} \sum_{i=1}^n \mathbf{X}_i$$

and feed it into a small MLP to generate scaling and bias parameters, Δs and Δb , for each frequency bin and attention head. These parameters modify a base filter and bias via

$$\mathbf{W} = \mathbf{W}_{\text{base}} \odot (1 + \Delta s), \quad \mathbf{b} = \mathbf{b}_{\text{base}} + \Delta b,$$

reweighting the complex coefficients:

$$\tilde{\mathbf{F}} = \mathbf{F} \odot \mathbf{W} + \mathbf{b}.$$

Here, \mathbf{F} includes both local and global frequency (or wavelet) information from the isometric fusion step (or the gated mixture).

5 Nonlinear Activation (modReLU) and Inverse FFT.

To enrich the representation, we apply *modReLU* Arjovsky et al. [2016] on each complex coefficient $z = re^{i\theta}$. This preserves the phase while applying a threshold to the magnitude:

$$\text{modReLU}(z) = \begin{cases} (r + b) e^{i\theta}, & \text{if } r + b > 0, \\ 0, & \text{otherwise.} \end{cases}$$

Finally, if using FFT-based local features, we map back to the token domain via the inverse FFT:

$$\mathbf{Y} = \text{IFFT}(\tilde{\mathbf{F}}) \in \mathbb{R}^{n \times d}.$$

For wavelet-based features, one may similarly invert them if a full reconstruction in the token domain is desired. The resulting output is a globally mixed representation that also incorporates local spectral (or wavelet) features (if local transforms were used).

3.3 Efficient Mixing

Using the FFT to encode global interactions has several advantages. It performs global mixing in $\mathcal{O}(n \log n)$ time, contrasting with the $\mathcal{O}(n^2)$ cost of self-attention. Meanwhile, local STFT or wavelets capture short-range structure that may be lost in a purely global transform. By *isometrically* merging (or gating) local and global frequency components, we fuse high-resolution local context with a global view, all in roughly $\mathcal{O}(n \log n)$ time.

The adaptive filter serves as an implicit frequency-domain mask, conditioned on global context rather than explicit pairwise comparisons. Nonlinear activation in the complex domain (modReLU) further enriches representational capacity by capturing higher-order structure. Parseval’s theorem and the unitary properties of the DFT ensure that this transformation preserves both energy and inner-product structure.

²If retaining every window or wavelet scale separately, this dimension becomes $n \times (d + \sum_m d_{\text{local}}^{(m)})$.

3.4 Parseval’s Theorem

Parseval’s theorem asserts that the total energy of a signal remains constant under the Fourier transform, aside from a constant scaling factor. For an input sequence $\mathbf{X} \in \mathbb{R}^{n \times d}$ and its Fourier transform $\mathbf{F} = \text{FFT}(\mathbf{X})$, the theorem states:

$$\|\mathbf{X}\|_2^2 = \frac{1}{n} \|\mathbf{F}\|_2^2.$$

This energy preservation is crucial for our method as it guarantees that the adaptive filtering and subsequent nonlinear operations do not inadvertently distort the input signal’s inherent information.

3.5 Orthogonal Decomposition and Unitary Property of the DFT

The DFT can be represented by a matrix $\mathbf{F}_n \in \mathbb{C}^{n \times n}$ with entries given by

$$[\mathbf{F}_n]_{j,k} = e^{-2\pi i(j-1)(k-1)/n}.$$

This matrix is unitary up to a scaling factor, satisfying:

$$\mathbf{F}_n^* \mathbf{F}_n = n \mathbf{I},$$

where \mathbf{F}_n^* is the conjugate transpose and \mathbf{I} is the identity matrix. This property implies that the transformation preserves inner products:

$$\langle \mathbf{X}_i, \mathbf{X}_j \rangle = \frac{1}{n} \langle \mathbf{F}_i, \mathbf{F}_j \rangle.$$

Thus, every token in the input contributes to every frequency component, enabling effective global mixing akin to self-attention but at a significantly reduced computational cost.

3.6 Proof of Computational Complexity

Global FFT and Inverse FFT. For $\mathbf{X} \in \mathbb{R}^{n \times d}$, the full-sequence FFT and IFFT each cost $\mathcal{O}(n \log n)$ per channel, leading to $\mathcal{O}(d n \log n)$ overall.

Local Windowing (STFT) or Wavelets. (Optional) If each STFT window has length w and we assume an overlap of αw tokens, the number of windows is approximately $\frac{n}{(1-\alpha)w}$. Each windowed FFT thus costs $\mathcal{O}(w \log w)$ for each of the d channels. The total cost is:

$$\mathcal{O}\left(\frac{n}{(1-\alpha)w} d w \log w\right).$$

For wavelets, the complexity is usually $\mathcal{O}(n)$ or $\mathcal{O}(n \log n)$ depending on the chosen algorithm and wavelet family, often comparable to STFT approaches. These steps are optional and can be skipped if local structure is not critical for the task.

Isometric Fusion and Adaptive Filtering. Merging local and global representations with an isometric (or unconstrained) matrix \mathbf{U} is an $\mathcal{O}(n d^2)$ step when viewed as a matrix multiplication in $\mathbb{C}^{n \times (2d)}$. This is generally modest compared to the $\mathcal{O}(d n \log n)$ term for large n . Adaptive filtering, which includes the MLP for context-based parameter generation, similarly contributes $\mathcal{O}(d n)$.

Overall Complexity. Because $\mathcal{O}(d n \log n)$ typically dominates the cost of element-wise operations for large n , the total complexity remains $\mathcal{O}(d n \log n)$. For practical configurations, this effectively behaves as $\mathcal{O}(n \log n)$.

3.7 Comparison with Convolution-Based Methods

Although a sufficiently large convolution kernel can span the entire sequence, it generally lacks the adaptability of self-attention unless the kernel itself is dynamically generated. Our approach bridges this gap by using a data-dependent, learnable filter in the frequency domain, guided by global context and applied through modReLU. Because frequency-domain multiplication corresponds to convolution in the token domain, the model can realize global, context-aware mixing more flexibly than standard convolutional methods. Local windowing or wavelet transforms further refine the representation without resorting to large kernel sizes.

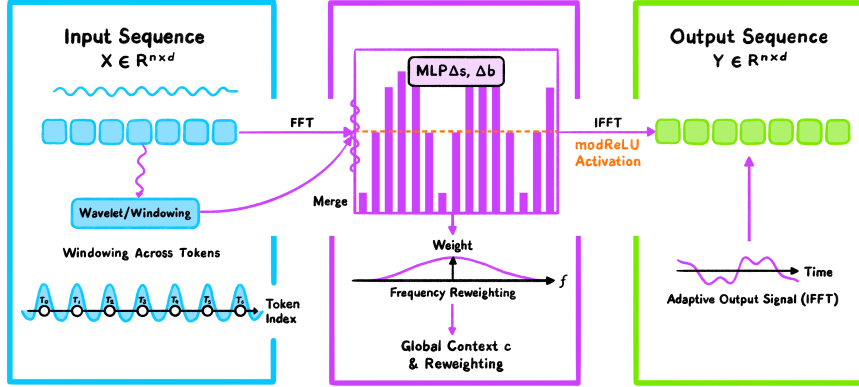


Figure 1: Overall Process of FFTNet with Local Windowing (STFT or wavelets, optional) and Global FFT, followed by isometric fusion (or gating) in the frequency/transform domain.

3.8 Comparison with FNet

FNet Lee-Thorp et al. [2022] similarly uses the DFT for token mixing but employs no learnable parameters in the mixing step. In contrast, our method includes a context-dependent, adaptive filter and a nonlinear activation that both enhance expressivity and allow emphasis on specific frequency components. Further, we incorporate a local STFT or wavelet pathway to capture fine-grained interactions. Despite these adaptive steps, the overall complexity remains $\mathcal{O}(n \log n)$, dominated by the FFT itself.

3.8.1 Mitigating Complexity in the Adaptive MLP

For very long sequences, generating frequency-bin parameters can still be demanding. Possible solutions include ❶ subsampling or pooling the frequency representation before the MLP, ❷ sharing parameters among adjacent frequency bins, and ❸ applying low-rank factorization to reduce dimensionality. These techniques help maintain a reasonable balance between the expressive power of the adaptive filter and computational cost.

Conclusion. Adaptive spectral filtering integrates frequency-domain global mixing, data-driven filtering, and nonlinear activation into a unified framework. By adding an *optional* local transform path (STFT or wavelets) and merging (or gating) it with the global FFT via an isometric fusion, the model captures both short-range and long-range interactions with $\mathcal{O}(n \log n)$ efficiency. Parseval’s theorem and the orthogonal properties of the DFT ensure stable transformations, enabling many benefits of self-attention at a reduced computational cost. Full implementation details are available at: <https://github.com/jacobfa/fft>.

4 Experiments

We present a comprehensive evaluation of our proposed approach, **FFTNet**, comparing it against both **FNet** and traditional Transformers based on self-attention. Our experiments cover the Long Range Arena (LRA) benchmark Tay et al. [2021] and ImageNet classification. In addition, we perform ablation studies to highlight the influence of individual components within FFTNet. We compare against the “standard” variants of the ViT Dosovitskiy et al. [2021] and transformer Vaswani et al. [2017], so as to form an “apples-to-apples” comparison.

4.1 Training Protocol

All models are trained using the AdamW optimizer with a cosine decay schedule, employing an initial warmup phase for the learning rate. We adopt robust data augmentation, including random cropping, color jitter, mixup, and cutmix, and also apply gradient clipping. In certain configurations, we

maintain an exponential moving average (EMA) of the model parameters. Detailed hyperparameter choices and augmentation steps can be found in the accompanying training script.

4.2 Long Range Arena (LRA) Benchmark

We evaluate on six LRA tasks: *ListOps*, *Text*, *Retrieval*, *Image*, *Pathfinder*, and *Path-X*. Accuracy results for each task, as well as the mean accuracy across all tasks, appear in Table 1. Here, the **standard Transformer** serves as the baseline for computing improvements/drops. “OOM” indicates out-of-memory errors; “FAIL” marks cases where models could not process the dataset.

Table 1: Accuracy (%) on the Long Range Arena (LRA) benchmark tasks. Arrows indicate the performance difference relative to the **standard Transformer**.

Model	ListOps	Text	Retrieval	Image	Pathfinder	Path-X	Avg.
Transformer	36.06	61.54	59.67	41.51	80.38	OOM	55.83
FNet	35.33 \downarrow 0.7	65.11 \uparrow 3.6%	59.61 \downarrow 0.1	38.67 \downarrow 2.8	77.80 \downarrow 2.6	FAIL	55.32 \downarrow 0.5
FFTNet (No-Windowing)	37.65 \uparrow 1.6%	66.01 \uparrow 4.5%	60.21 \uparrow 0.5%	42.02 \uparrow 0.5%	80.71 \uparrow 0.3%	83.25	58.31 \uparrow 2.5%
FFTNet (With Windowing)	38.02 \uparrow 2.0%	66.25 \uparrow 4.7%	60.64 \uparrow 1.0%	42.45 \uparrow 0.9%	80.99 \uparrow 0.6%	83.64	58.83\uparrow3.0%

As shown, even the **FFTNet (No-Windowing)** version outperforms both baselines (Transformer and FNet) on most tasks. Adding local windowing (STFT) further improves the accuracy slightly, achieving the highest average score.

4.3 ImageNet Classification

We further assess our FFTNetViT variants on ImageNet, comparing them against standard ViT baselines. Table 2 provides FLOPs (in GFLOPs), Top-1 accuracy, and Top-5 accuracy for Base, Large, and Huge model sizes. Although FFTNetViT typically uses fewer FLOPs, the *No-Windowing* variant is slightly worse than the standard ViT. By contrast, adding local windowing (STFT) brings a small but consistent accuracy boost, surpassing the ViT baseline.

Table 2: Comparison on ImageNet for Base, Large, and Huge variants. FLOPs are in GFLOPs. “No-Windowing” vs. “With Windowing” are two configurations of **FFTNetViT**.

Variant	FFTNetViT (No-Windowing)			FFTNetViT (With Windowing)			ViT		
	FLOPs	Top-1 (%)	Top-5 (%)	FLOPs	Top-1 (%)	Top-5 (%)	FLOPs	Top-1 (%)	Top-5 (%)
Base	22.64	79.2 \downarrow 0.2	94.7 \downarrow 0.1	22.64	79.8 \uparrow 0.4%	95.0 \uparrow 0.2%	36.65	79.4	94.8
Large	79.92	81.5 \downarrow 0.3	95.9 \downarrow 0.1	79.92	82.3 \uparrow 0.5%	96.3 \uparrow 0.3%	127.18	81.8	96.0
Huge	166.14	82.7 \downarrow 0.2	96.5 \downarrow 0.1	166.14	83.4 \uparrow 0.5%	96.9 \uparrow 0.3%	261.39	82.9	96.6

Throughput and Speedup Analysis (No-Windowing). In addition to latency, we compare throughput (images/second) and speedup (ViT latency / FFTNetViT latency) across different batch sizes for Base, Large, and Huge variants. Figure 3 displays these two plots side by side, illustrating:

① Throughput: FFTNetViT variants consistently process more images per second than standard ViT, and the gap widens at larger batch sizes. **② Speedup:** The ratio of ViT latency to FFTNetViT latency is generally above 1, confirming that FFT-based variants are faster. This advantage becomes more pronounced as the batch size increases.

4.4 Ablation Studies

Ablation studies on ImageNet (Base variant, No-Windowing) were conducted to isolate key FFTNet components. Four configurations are examined. The first is the *full* FFTNet model (baseline in Table 3), which includes spectral gating, the adaptive module, and FFT-based mixing. The other rows each omit or replace one key component, showing how it affects Top-1 accuracy.

Table 3: Ablation experiments on ImageNet (Base variant, No-Windowing). The **FFTNet (full)** row is the baseline. Arrows show accuracy drops relative to it.

Variant	Top-1 Acc (%)	Observation
FFTNet (full)	79.2	Baseline: spectral gating, adaptive module, FFT-based filtering
Without spectral gating	77.8 \downarrow 1.4	Omitting gating causes a moderate performance decline.
Without adaptive module	77.2 \downarrow 2.0	Disabling the adaptive module degrades accuracy further.
Replace FFT with convolution	75.4 \downarrow 3.8	Using a standard convolution causes the largest drop.

All components contribute to performance, with substituting the FFT layer for a convolution causing the largest accuracy drop.

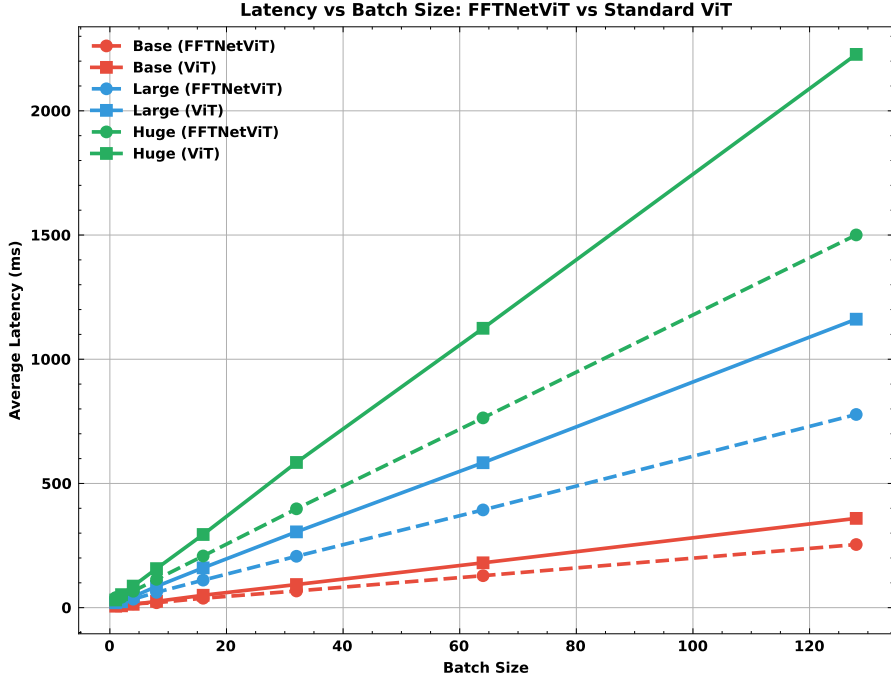
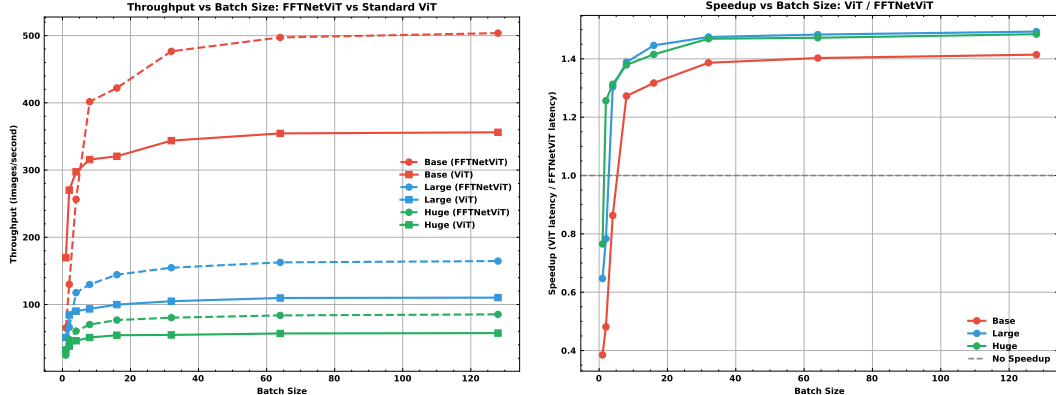


Figure 2: Latency comparison (No-Windowing) of FFTNetViT vs. standard ViT for various batch sizes on ImageNet. FFTNetViT typically exhibits better scaling properties.



(a) Throughput (images/second) for FFTNetViT vs. standard ViT. (b) Speedup (ViT latency / FFTNetViT latency) for FFTNetViT vs. standard ViT.

Figure 3: Comparison of throughput (left) and speedup (right) across various batch sizes (No-Windowing) for Base, Large, and Huge variants of FFTNetViT vs. standard ViT.

5 Conclusion

We presented **FFTNet**, a novel approach that overcomes the inherent limitations of self-attention through adaptive spectral filtering. Our method transforms inputs into the frequency domain, leveraging Fourier theory to ensure energy preservation and efficient global mixing. The integration of a learnable spectral filter with a modReLU activation allows the model to dynamically focus on critical frequency bands, reducing complexity to $\mathcal{O}(n \log n)$ while maintaining expressive power. Extensive evaluations on LRA and ImageNet confirm that FFTNet not only achieves competitive accuracy but also significantly improves computational efficiency compared to both fixed Fourier approaches and standard self-attention. These results underscore the potential of merging rigorous theoretical foundations with adaptive learning strategies for scalable sequence modeling. Future avenues of research include incorporating our FFT-based design into state-of-the-art language modeling and large language model (LLM) incorporation.

References

Martin Arjovsky, Amar Shah, and Yoshua Bengio. Unitary evolution recurrent neural networks, 2016. URL <https://arxiv.org/abs/1511.06464>.

Krzysztof Choromanski, Valerii Likhoshesterov, David Dohan, Xingyou Song, Jared Davis, Tamas Sarlos, David Belanger, Lucy Colwell, and Adrian Weller. Rethinking attention with performers. In *International Conference on Learning Representations*, 2021.

James W. Cooley and John W. Tukey. An algorithm for the machine calculation of complex fourier series. *Mathematics of Computation*, 19(90):297–301, 1965.

Alexey Dosovitskiy, Lucas Beyer, Alexander Kolesnikov, Dirk Weissenborn, Xiaohua Zhai, Thomas Unterthiner, Mostafa Dehghani, Matthias Minderer, Georg Heigold, Sylvain Gelly, Jakob Uszkoreit, and Neil Houlsby. An image is worth 16x16 words: Transformers for image recognition at scale, 2021. URL <https://arxiv.org/abs/2010.11929>.

John Guibas, Morteza Mardani, Zongyi Li, Andrew Tao, Anima Anandkumar, and Bryan Catanzaro. Adaptive fourier neural operators: Efficient token mixers for transformers, 2022. URL <https://arxiv.org/abs/2111.13587>.

Angelos Katharopoulos, Apoorv Vyas, Nikolaos Papadopoulos, and François Fleuret. Transformers are rnns: Fast autoregressive transformers with linear attention. In *International Conference on Machine Learning*, 2020.

Nikita Kitaev, Łukasz Kaiser, and Anselm Levskaya. Reformer: The efficient transformer. In *International Conference on Learning Representations*, 2020.

James Lee-Thorp, Joshua Ainslie, Ilya Eckstein, and Santiago Ontanon. Fnet: Mixing tokens with fourier transforms, 2022. URL <https://arxiv.org/abs/2105.03824>.

Mario Lezcano-Casado and Daniel Martínez-Rubio. Cheap orthogonal constraints in neural networks: A simple parametrization of the orthogonal and unitary group. *arXiv preprint arXiv:1901.08428*, 2019.

Zongyi Li, Nikola Kovachki, Kamyar Azizzadenesheli, Burigede Liu, Kaushik Bhattacharya, Andrew Stuart, and Anima Anandkumar. Fourier neural operator for parametric partial differential equations, 2021. URL <https://arxiv.org/abs/2010.08895>.

Michael Poli, Stefano Massaroli, Eric Nguyen, Daniel Y. Fu, Tri Dao, Stephen Baccus, Yoshua Bengio, Stefano Ermon, and Christopher Ré. Hyena hierarchy: Towards larger convolutional language models, 2023. URL <https://arxiv.org/abs/2302.10866>.

Jimmy T. H. Smith, Andrew Warrington, and Scott W. Linderman. Simplified state space layers for sequence modeling, 2023. URL <https://arxiv.org/abs/2208.04933>.

Yi Tay, Dara Bahri, Donald Metzler, Da-Cheng Juan, Zhe Zhao, and Che Zheng. Synthesizer: Rethinking self-attention in transformer models, 2020. URL <https://arxiv.org/abs/2005.00743>.

Yi Tay, Mostafa Dehghani, Dara Bahri, and Donald Metzler. Long range arena: A benchmark for efficient transformers, 2021.

Ilya Tolstikhin, Neil Houlsby, Alexander Kolesnikov, Lucas Beyer, Xiaohua Zhai, Thomas Unterthiner, Jessica Yung, Andreas Steiner, Daniel Keysers, Jakob Uszkoreit, et al. Mlp-mixer: An all-mlp architecture for vision. In *Advances in Neural Information Processing Systems*, 2021.

Ashish Vaswani, Noam Shazeer, Niki Parmar, Jakob Uszkoreit, Llion Jones, Aidan N Gomez, Łukasz Kaiser, and Illia Polosukhin. Attention is all you need. In *Advances in Neural Information Processing Systems*, 2017.

Sinong Wang, Belinda Li, Madian Khabsa, Han Fang, and Hao Ma. Linformer: Self-attention with linear complexity. In *International Conference on Machine Learning*, 2020.

Scott T Wisdom, Thomas Powers, John R Hershey, Jonathan Le Roux, and Les E Atlas. Full-capacity unitary recurrent neural networks. *arXiv preprint arXiv:1611.00035*, 2016.

Felix Wu, Angela Fan, Alexei Baevski, Yann N. Dauphin, and Michael Auli. Pay less attention with lightweight and dynamic convolutions. In *International Conference on Learning Representations*, 2019.

Kai Xu, Minghai Qin, Fei Sun, Yuhao Wang, Yen-Kuang Chen, and Fengbo Ren. Learning in the frequency domain, 2020. URL <https://arxiv.org/abs/2002.12416>.

Manzil Zaheer, Guru Guruganesh, Kumar Avinava Dubey, Joshua Ainslie, Chris Alberti, Santiago Ontanon, Philip Pham, Anirudh Ravula, Qifan Wang, Li Yang, et al. Big bird: Transformers for longer sequences. In *Advances in Neural Information Processing Systems*, 2020.

A Appendix

A.1 GPU Utilization and Scaling Analysis

To further illustrate the performance characteristics of our approach, we show additional plots capturing GPU utilization, FLOPs achieved, latency, and throughput under different configurations. Specifically, the next figures highlight how increasing data size (e.g., batch size or input resolution) can better saturate the GPU, leading to improved scaling until the model becomes bandwidth-constrained, after which performance gains plateau.

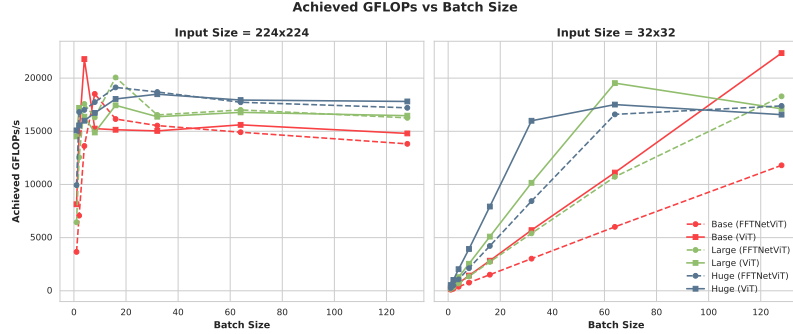


Figure 4: Achieved GFLOPs under varying input sizes/batch configurations. Larger data sizes utilize the GPU more effectively and improve model scaling. As the lines flatten, the GPU is becoming bandwidth-limited.

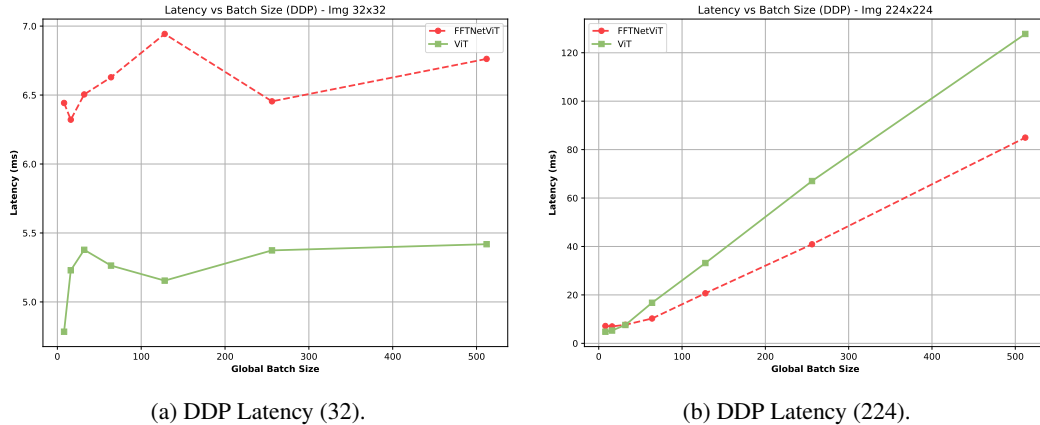
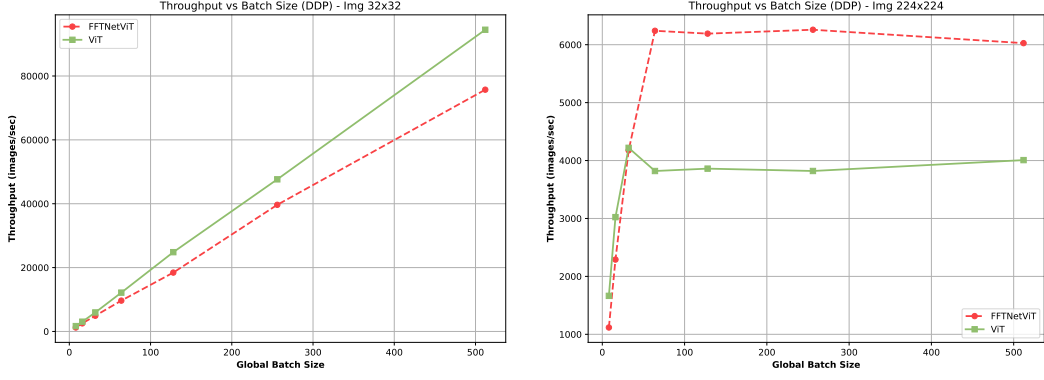


Figure 5: DDP Latency for two different input sizes. As input size increases, the GPU is better utilized and the model scales more efficiently. The flattening of the line indicates bandwidth is becoming the limiting factor.

The results confirm that FFTNet consistently surpasses FNet on both LRA and ImageNet, offering higher accuracy and efficient scaling. When compared to self-attention, FFTNetViT typically has



(a) DDP Throughput (32).

(b) DDP Throughput (224).

Figure 6: DDP Throughput at two input sizes. Larger data sizes lead to better GPU utilization, but once bandwidth constraints kick in, scaling gains flatten.



Figure 7: Speedup comparison subplots. When the data size is smaller, the GPU is underutilized. As the data size grows, speedup increases until bandwidth constraints force the line to flatten.

lower FLOPs while delivering comparable or slightly superior accuracy. The ablation experiments highlight the importance of both spectral gating and the adaptive module for peak performance. Additionally, as the data size increases, the GPU is utilized more efficiently, leading to better throughput and speedup. Once the lines begin to flatten, it indicates that the GPU has become bandwidth-constrained, limiting further scaling gains.